DYNAMIC STABILITY UNDER SUDDEN LOADS

G.J.Simitses

Aerospace Engineering and Engineering Mechanics
University of Cincinnati, Cincinnati, OH 45221-0070

ABSTRACT

The concept of dynamic stability of elastic structures subjected to sudden (step) loads is discussed. The various criteria and related methodologies for estimating critical conditions are presented with the emphasis on their similarities and differences. These are demonstrated by employing a simple mechanical model. Several structural configurations are analyzed, for demonstration purposes, with the intention of comparing critical dynamic loads to critical static loads. These configurations include shallow arches and shallow spherical caps, two bar frames, and imperfect cylindrical shells of metallic as well as laminated composite construction. In the demonstration examples, the effect of static preloading on the dynamic critical load is presented.

INTRODUCTION

Dynamic stability or instability of elastic structures has received considerable attention in the past thirty years. The beginning of the subject can be traced to the investigation of Koning et.al. [1], who considered the response of an imperfect (half-sine wave) simply supported column subjected to a sudden axial load of specified duration. Since then, several studies have been conducted by various investigators on structural systems, which are either suddenly loaded or subjected to time-dependent loads (periodic or non-periodic) and several attempts have been made to find common response features and to define critical conditions for these systems. As a result of this, the term "Dynamic Stability" encompasses many classes of problems, and many different physical phenomena. Therefore, it is not surprising that there exist several uses and interpretations of the term.

A large class of structural problems, that has received considerable attention and does qualify as a category of dynamic stability, is that of impulsively loaded configurations and configurations which are suddenly loaded with loads of constant magnitude and infinite duration. These configurations under static loading, are subject to either limit-point instability or bifurcational instability with unstable post-buckling branch (violent buckling).

Solutions to such problems started appearing in the literature in the early 1950's. Hoff et.al. [2] considered the dynamic stability of a pinned half-sine arch under a half-sine distributed load. Budiansky et.al. [3] in studying the axisymmetric behavior of a shallow spherical cap under suddenly applied loads defined the load to be critical when the transient response increases suddenly with very little increase in the magnitude of the load. This concept was adopted by numerous investigators [4] in the subsequent years, because it is tractable to computer solutions. Finally, the concept was generalized in a subsequent paper by Budiansky [5] in attempting to predict critical conditions for imperfection-sensitive structures under time-dependent loads.

Conceptually, one of the best efforts in the area of dynamic buckling, under suddenly applied loads, is the work of Hsu and his collaborators [6,7]. In his studies, he defined sufficiency conditions for stability and sufficiency conditions for instability, thus finding upper and lower bounds for the critical impulse or critical sudden load. Independently, Simitses [8] in dealing with the dynamic buckling of shallow arches and spherical caps termed the lower bound as a minimum possible critical load (MPCL) and the upper bound as a minimum guaranteed critical (MGCL). Finally, Thompson [9] presented a criterion for estimating critical conditions for suddenly-loaded systems.

FUNDAMENTAL CONCEPTS

The totality of concepts and methodologies used by the various investigators in estimating critical conditions for suddenly loaded elastic systems can be classified in the following three groups: (a) The Equations of Motion Approach [3]. The equations of motion are (numerically) solved for various values of the load parameter (ideal impulse, or sudden load), thus obtaining the system response. The load parameter, at which there exists a large (finite) change in the response, is called critical. (b) The Total Energy - Phase Plane Approach [6,7]. Critical conditions are related to characteristics of the system phase-plane, and the emphasis is on establishing sufficient conditions for stability (lower bounds) and instability (upper bounds). (c) The Total Potential Energy Approach [2,8]. Critical conditions are related to characteristics of the system total potential. Through this approach also, lower and upper bounds of critical conditions are established. This last approach is applicable to conservative systems only. The common concept in all three approaches is that there exists dynamic stability, if the motion resulting from the sudden application of the loads is bounded. Of course, one must exercise special care in establishing allowable bounds for the

resulting motion. These concepts and the related methodologies will be discussed, during the presentation, through a simple mechanical model. The interested reader is referred to [4].

APPLICATIONS

In this section, results are presented for a few structural elements and configurations. The sudden loads are step loads of constant magnitude and finite duration, including the extreme cases of ideal impulse and constant load of infinite duration. The oral presentation includes a half-sine sudden load, an eccentrically loaded two bar frame and a shallow spherical cap. For all of these elements, the construction material is a metal. For details, see [4].

In addition, results are presented for metallic and laminated cylindrical shells, subjected to suddenly applied uniform axial compression and bending moment (individual application). Moreover, results are presented for laminated cylindrical shells, subjected to suddenly applied external pressure. The motivation for these studies is the physical relevance of dynamic loads during the service of aircraft, surface ships, submarines and jet engine casings. The nature and source of these loads could be attributed to gusts, blasts, high sea waves and the loss of one or more blades during the operation of a jet engine (blade out).

Metallic Cylinders

Consider a metallic cylinder, subjected to either uniform axial compression or bending moment, which are suddenly applied. The thin cylindrical shell is imperfect and the material and geometric properties are:

$E = 72.4(10^9)$ Pa, $\mu = 0.3$, $R = L = 0.1016$ m, $t = 0.1016(10^{-3})$m, and

$$w^{\circ}(x,y) = at\left(-\cos\frac{2\pi x}{L} + 0.1\sin\frac{\pi x}{L}\cos n\theta\right)$$

where E is Young's modulus, μ is Poisson's ratio, R, L and t are the radius, length and thickness, respectively, and w^0 the initial geometric imperfection. Note that $a = w^{\circ}_{\max}/t$. Fig. 1 depicts dynamic compression critical loads versus duration time for two imperfection amplitudes. For more results and details, see [10].

Laminated Cylinders

The next application is a laminated cylindrical shell made out of Boron/Epoxy under the same loads with the following properties: $E_{11} = 206.9\ (10^9)$Pa; $E_{22} = E_{33} = 18.62\ (10^9)$ Pa; $G_{12} = G_{13} = 4.48\ (10^9)$ Pa; $E_{23} = 2.556\ (10^9)$ Pa; $\mu_{12} = \mu_{13} = 0.21$; $\mu_{13} = 0.45$; $R = L = 0.1905$m; $h_{ply} = 1.346(10^{-3})$ m; $\left(45^{\circ}/-45^{\circ}\right)_s$ and $w^{\circ}(x,y) = at\sin\left[7\pi\left(\frac{x}{2} - \frac{1}{2}\right)\right]\cos 4\theta$. Fig. 2 depicts dynamic critical loads versus duration time, T and a = 0.5. For more details see [10].

Finally, results are presented herein for laminated, imperfect, composite shells subjected to "step" external pressure with and without static preloading. Because of space limitations, limited results are shown on this paper. The lecture will provide greater detail. The construction material for these cylindrical shells is Graphite/Epoxy and material and geometric properties are: $\rho = 1.6\ (10^3)$ Kg/m^3; $E_{11} = 136.9$ GPa; $E_{22} = E_{33} = 9.86$ GPa; $G_{12} = G_{13} = 5.65$ GPa; $G_{23} = 2.69$ GPa; $\mu_{12} = \mu_{13} = 0.293$; $\mu_{23} = 0.45$; $R = 17.78$cm; $h_{ply} = 0.1778$mm; L/R = 2,3,5; $\left(90^0_i/0^0_i\right)_s$, i=2,3,4&5; ; $\left(45^{\circ}/-45^{\circ}\right)_s$ and $\left(0^0_s/90^0_s\right)_s$. $\xi = 0.01, 0.05$ *and* 0.10

$\left(w^{\circ}_{\max} = 0.08763mm, 0.43815mm \text{ and } 0.8763mm\right)$

A finite element code for thick shells was employed (in ABAQUS) and both implicit and explicit time integration methods were used. Results were generated by employing all three methods discussed earlier. Details of the employed solution methodology can be found in [11].

Fig. 3 depict critical pressures in psi versus duration time in microseconds for $\left(90^0_s/0^0_s\right)_s$, and L/R = 2,3,5. Note that as the cylinder length increases the difference between the static critical pressure and the dynamic critical pressure (for infinite duration) decreases. Fig. 4 depicts the effect of static preloading for the same configurations as in Fig. 3. The oral presentation will contain more results.

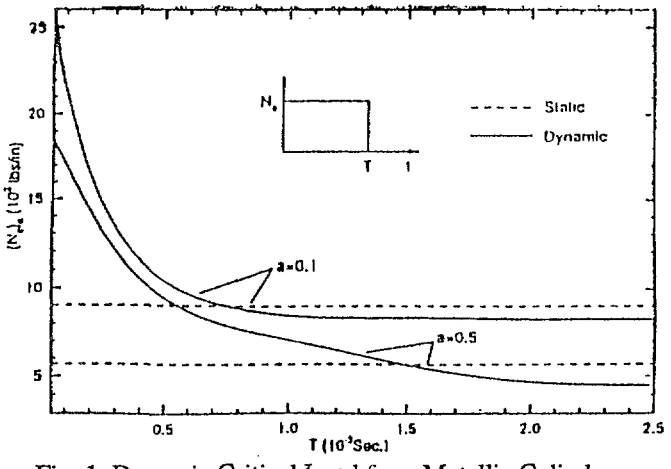

Fig. 1. Dynamic Critical Load for a Metallic Cylinder

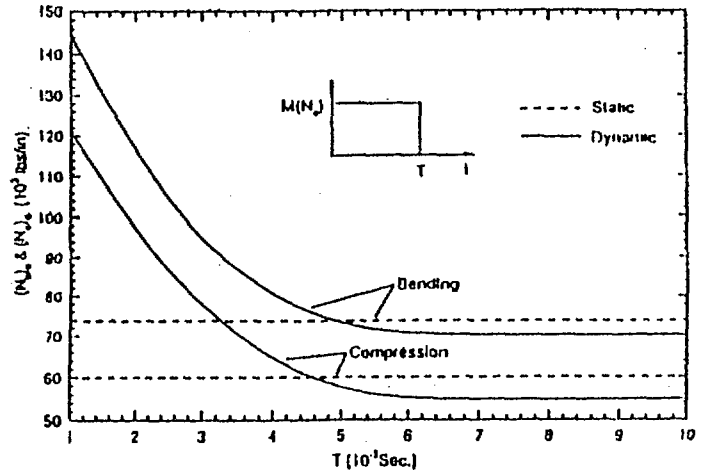

Fig. 2. Dynamic Critical Load for a Laminated Cylinder

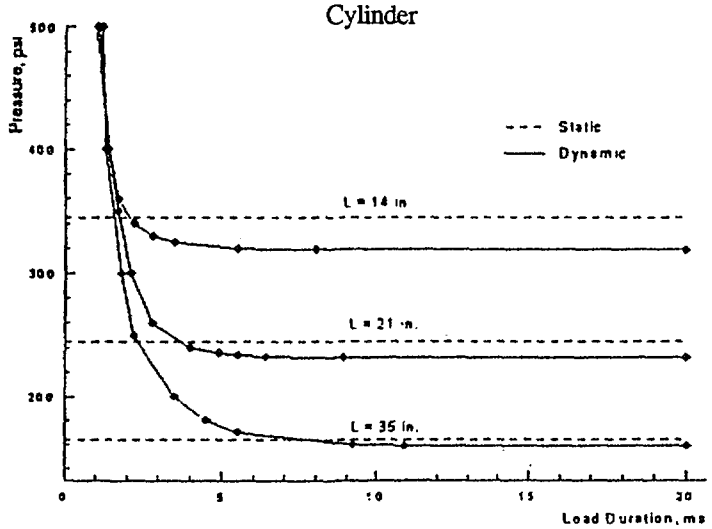

Fig. 3. Static and Dynamic Critical Pressure

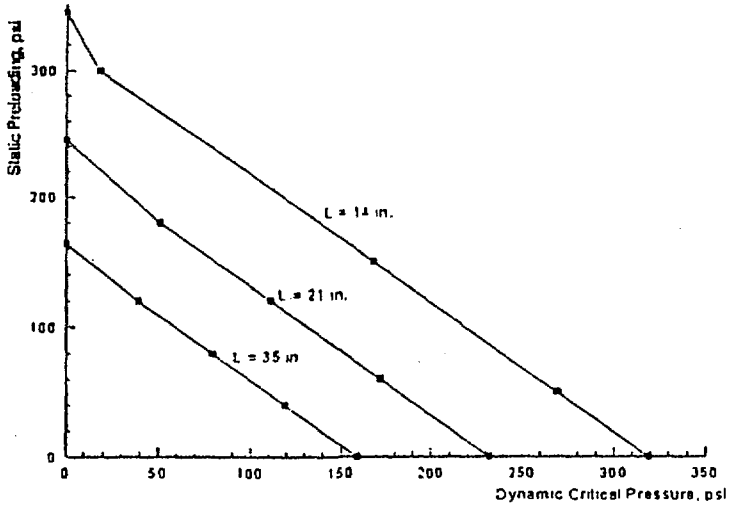

Fig. 4. Effect of Static Preloading

ACKNOWLEDGMENTS

Part of the work was supported by AFOSR and part by ONR. Their financial assistance is gratefully acknowledged. Moreover thanks are due to my research collaborators, Drs. A.N. Kounadis, I. Sheinman, J. Giri, C. Lazopoulos, D. Shaw, A. Tabiei and R. Tanov.

REFERENCES

1. Koning, C., and Taub, J., "Impact Buckling of Thin Bars in the Elastic Range Hinged at Both Ends", Luftfahrtforschung, Vol. 10, No.2, 1933, pp. 55-64, (translated as NACA TM 748 in 1934).
2. Hoff, N.J., and Bruce, V.C., "Dynamic Analysis of the Buckling of Laterally Loaded Flat Arches", Quart. Math and Phys., Vol. 32, 1954, pp. 276-388.
3. Budiansky, B., and Roth, R.S., "Axisymmetric Dynamic Buckling of Clamped Shallow Spherical Shells," Collected Papers on Instability of Shell Structures, NASA TN D-1510, 1962.
4. Simitses, G.J., Dynamic Stability of Suddenly Loaded Structures. Springer-Verlag, New York, 1989.
5. Budiansky, B., "Dynamic Buckling of Elastic Structures: Criteria and Estimates" in Dynamic Stability of Structures. (edited by G. Herrman), Pergamon Press, New York, 1967.
6. Hsu, C.S., "The Effects of Various Parameters on the Dynamic Stability of a Shallow Arch, J. Appl. Mech., Vol. 34, No. 2, 1967, pp. 349-356.
7. Hsu, C.S., "Stability of Shallow Arches Against Snap-Through Under Timewise Step Loads," J. Appl. Mech., Vol. 35, No.1, 1968, pp.31-39.
8. Simitses, G.J., "Dynamic Snap-Through Buckling of Low Arches and Shallow Spherical Caps", Ph.D. Dissertation, Department of Aeronautics and Astronautics, Stanford University, June 1965.
9. Thompson, J.M.T., "Dynamic Buckling Under Step Loading", Dynamic Stability of Structures (edited by G. Herrman), Pergamon Press, N.Y., 1967.
10. Huyan, X. and Simitses, G.J. "Dynamic Buckling of Imperfect Cylindrical Shells Under Axial Compression and Bending Moment," AIAA J., Vol. 35, No.8, 1997, pp.1404-1412.
11. Tabiei, A., Tanov, R. and Simitses, G.J., "Numerical Simulation of Cylindrical Laminated Shells Under Impulsive Lateral Pressure," AIAA Paper 98-1762, April, 1998.

SUPPRESSION OF LARGE SPAN WINGS FLUTTER BY AUTOMATIC PILOT

By Raphael Cohen* Robert Zickel and Oded Yehezkely
RAFAEL P.O.B. 2250 Haifa
*Conference Lecturer

Abstract

In this work, flutter of large span wings is analyzed. The flutter phenomenon, in this case, is a result of the coupling between the bending vibrations of the wings and the pitch oscillations of the body due to the aerodynamic forces. A simple mathematical model of the system is constructed. The model includes a central rigid body and two symmetric rigid wings which have an angular degree of freedom to model their bending. Aerodynamic forces and moments are applied to the body and the wings. Torque proportional to the bending angle is applied between the body and each of the wings. The equations of motion of the system are developed with the aid of the *Autolev* software. Simulation carried out with these equations enables diagnosis of the conditions for flutter. It is found that this flutter phenomenon depends on the geometric relations, flight velocity and wings rigidity. Linearization of the equations of motion demonstrates that flutter of wings is an instability which is characterized by the positive real value of one of the eigenvalues of the system. Adding control forces which are produced by the automatic pilot and are applied by control surfaces deflection eliminates the flutter phenomenon in all practical cases.

Introduction

This work deals with flutter properties of an aircraft having four degrees of freedom (DOF); vertical up-down movement, pitch and two wings bending. The flutter analysis is done for uncontrolled and for pitch - controlled aircraft. The analysis method combines an aeroelastic model with a control model for time-domain simulations.

This work can be compared to the classic case of flutter of wings having two DOF which was analyzed by Hancock [1]. Hancock deals with flutter as a result of coupling between bending and torsion of the wings. In the present work the flutter due to coupling between the pitch of the aircraft and the bending of its wings is addressed, while the wings are assumed to be rigid in torsion.

The case of a missile controlled by pneumatically activated fins was analyzed by Yehezkely and Karpel [2] .In [2] only an open-loop control was analyzed while in the present work a closed-loop auto-pilot control is considered.

The present work combines both simulation of the nonlinear equations of motion together with analysis of the eigenvalues of the system after linearization. In the first part, the system without the auto-pilot control forces is analyzed. The dependence between the system parameters and the flutter phenomenon is investigated and presented.

In the second part of the work, the influence of control forces which are produced by the automatic pilot is analyzed. These forces are applied by control surfaces deflection at the rear part of the body. Addition of these control forces changes the aerodynamic behavior of the body and the flutter properties of the aircraft.

The Model

Figure 1 describes a model of a body wing aircraft type system. The model includes the following elements: central rigid body (A) and two symmetric rigid wings, (B) and (C). The body (A) has two DOF; a linear DOF Z in the vertical direction and an angular DOF α for the pitch. For simplicity it is assumed that the main body has a planar motion with constant velocity V in the horizontal direction ($\boldsymbol{n}_1$).

The wings (B) and (C), which are connected to the central body by angular flexible joints, have an angular DOF, q_b and q_c respectively, to model the wings bending. The bending flexibility of wings B and C with respect to the body A is modeled by torsion springs connecting B and C to A.

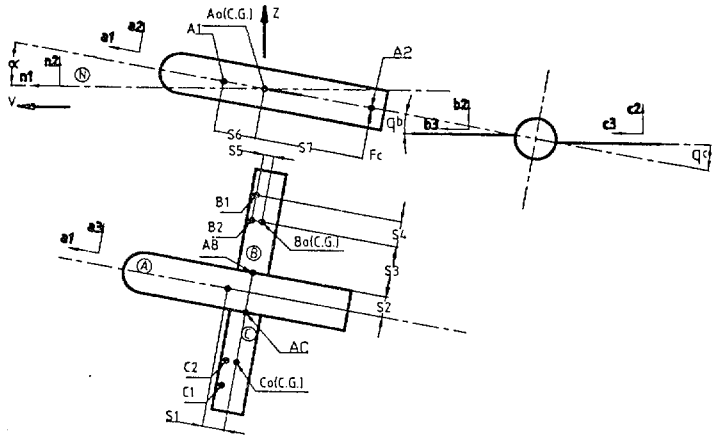

Fig.1: System configuration

Equations of Motion

To deal with the current flutter problem, the following frames are defined. $\boldsymbol{a}_i$, $\boldsymbol{b}_i$, $\boldsymbol{c}_i$ and $\boldsymbol{n}_i$ (i = 1,2,3) are sets of three dextral, mutually perpendicular unit vectors, fixed in A, B, C, and N (Newtonian reference frame) respectively, directed as described in figure 1. Two DOF are imposed on the body A, according to the above mentioned assumptions, one linear DOF in the vertical $\boldsymbol{n}_2$ direction and an angular DOF α (pitch) about $\boldsymbol{n}_3$. Two other DOF represent the bending of the wings B and C about A with angles q_B and q_C. Four generalized speeds are required to describe the motion of the system in N. The first two may be defined as:

$$u_1 \triangleq {}^N\boldsymbol{v}^{A_o} \cdot \boldsymbol{n}_1 = \dot{z} \qquad (1)$$

$$u_2 \triangleq {}^N\boldsymbol{\omega}^{A} \cdot \boldsymbol{a}_3 = \dot{\alpha} \qquad (2)$$

where ${}^N\boldsymbol{v}^{A_o}$ is the velocity of the mass center A_o of A in N, ${}^N\boldsymbol{\omega}^{A}$ is the angular velocity of A in N, α is the pitch angle and $\dot{\alpha}$ its time derivative. In addition, the

other two generalized speeds of the system may be defined as:

$$u_3 \triangleq - {}^A\omega^B \cdot \boldsymbol{a}_3 = \dot{q}_B$$
$$u_3 \triangleq + {}^A\omega^B \cdot \boldsymbol{a}_3 = \dot{q}_C \quad (3)$$

where ${}^A\omega^B$ and ${}^A\omega^C$ are respectively, the angular velocities of B and C relative to A, and q_B and q_C are the bending angles of B and C.

The generalized inertia forces may be formulated after expressing the terms for ${}^N\omega^B$ and ${}^N\omega^C$, the angular velocities of B and C in N and ${}^N\mathrm{v}^{B_o}$ and ${}^N\mathrm{v}^{C_o}$, the velocities of Bo and Co, the mass centers of B and C, in N. Now from equations (2) and (3):

$${}^N\omega^B = {}^N\omega^A + {}^A\omega^B = u_2\boldsymbol{a}_3 - u_3\boldsymbol{a}_1 \quad (4)$$

$${}^N\omega^C = {}^N\omega^A + {}^A\omega^C = u_2\boldsymbol{a}_3 + u_4\boldsymbol{a}_1 \quad (5)$$

Next, by defining the following position vectors from Ao to Bo and Co (see fig. 1):

$$\boldsymbol{p}^{A_o/AB} = -s_1\boldsymbol{a}_1 + s_2\boldsymbol{a}_3 \quad (6)$$
$$\boldsymbol{p}^{AB/B_o} = s_3\boldsymbol{b}_3 \quad (7)$$
$$\boldsymbol{p}^{A_o/AC} = -s_1\boldsymbol{a}_1 - s_2\boldsymbol{a}_3 \quad (8)$$
$$\boldsymbol{p}^{AC/C_o} = -s_3\boldsymbol{c}_3 \quad (9)$$

then with Eq. (1)

$${}^N\boldsymbol{v}^{A_o} = V\boldsymbol{a}_1 + u_1\boldsymbol{a}_2 \quad (10)$$

$${}^N\boldsymbol{v}^{AB} = {}^N\boldsymbol{v}^{A_o} + {}^N\omega^A \times \boldsymbol{p}^{A_o/AB}$$
$${}^N\boldsymbol{v}^{AC} = {}^N\boldsymbol{v}^{A_o} + {}^N\omega^A \times \boldsymbol{p}^{A_o/AC} \quad (11)$$

$${}^N\boldsymbol{v}^{B_o} = {}^N\boldsymbol{v}^{AB} + {}^N\omega^B \times \boldsymbol{p}^{AB/B_o}$$
$${}^N\boldsymbol{v}^{C_o} = {}^N\boldsymbol{v}^{AC} + {}^N\omega^B \times \boldsymbol{p}^{AC/C_o} \quad (12)$$

Using equations (10),(11) and (12) and defining the direction cosines between $\boldsymbol{n}_i, \boldsymbol{a}_i$ and $\boldsymbol{b}_i$ and between $\boldsymbol{n}_i, \boldsymbol{a}_i$ and $\boldsymbol{c}_i$ (I=1,2,3), leads to the required expressions for the evaluation of the inertia forces, partial angular velocities and partial velocities. Kane's formulation [3] can now be adapted to derive expressions for generalized inertia forces.

The active forces and torque are as follows:

1. The following aerodynamic forces and torque are assumed:

1.1 Normal force on the main body (A), at the point A1, due to the pitch angle α:

$$\mathbf{F}_1^{A1} = Q_d S_r C_{l\alpha}^{body} \alpha \mathbf{a}_2 \quad (13)$$

1.2 Normal force on the main body, due to the vertical velocity $\dot{z}$, at A1:

$$\mathbf{F}_2^{A1} = Q_d S_r C_{l\alpha}^{body} (\dot{z}/V)\mathbf{a}_2 \quad (14)$$

1.3 Pitch damping torque on (A):

$$\mathbf{T}^A = Q_d S_r C_r (C_r/2V) C_{mq} \dot{\alpha} \mathbf{a}_3 \quad (15)$$

where $Q_d = 0.5\rho V^2$, ρ is the air density, S_r and C_r are the reference area and length, $C_{l\alpha}^{body}$ and C_{mq} are the body lift slope and the pitch torque damping coefficients.

2. On the wings (B) and (C) the following forces and torque are applied:

2.1 Normal force due to the pitch angle α, acting at the control points B2 and C2 of wings B and C, respectively:

$$\mathbf{F}_1^{B2} = Q_d S_r C_{l\alpha}^{wing} \alpha \mathbf{b}_2$$
$$\mathbf{F}_1^{C2} = Q_d S C_{l\alpha}^{wing} \alpha \mathbf{c}_2 \quad (16)$$

2.2 Damping force due to the pitch rate $\dot{\alpha}$ at B2 and C2:

$$\boldsymbol{F}_2^{B2} = Q_d S_r C_{l\alpha}^{wing} [(s1 - s5)\dot{\alpha}/V]\boldsymbol{b}_2$$
$$\boldsymbol{F}_2^{C2} = Q_d S_r C_{l\alpha}^{wing} [(s1 - s5)\dot{\alpha}/V]\boldsymbol{c}_2 \quad (17)$$

2.3 Normal damping force due to the vertical velocity of the body $\dot{z}$:

$$\mathbf{F}_3^{B2} = Q_d S_r C_{l\alpha}^{wing} (\dot{z}/V)(-\mathbf{b}_2)$$
$$\mathbf{F}_3^{B2} = Q_d S_r C_{l\alpha}^{wing} (\dot{z}/V)(-\mathbf{c}_2) \quad (18)$$

2.4 Normal damping force due to the bending rate $\dot{q}_B$ on the point B1 of wing B and $\dot{q}_C$ on point C1 of wing C:

$$\mathbf{F}_4^{B1} = Q_d S_r C_{l\alpha}^{wing} (\dot{q}_B/V)(s_3 + s_4)(-\mathbf{b}_2)$$
$$\mathbf{F}_4^{C1} = Q_d S_r C_{l\alpha}^{wing} (\dot{q}_C/V)(s_3 + s_4)(-\mathbf{c}_2) \quad (19)$$

where $C_{l\alpha}^{wing}$ is the lift slope coefficient for each wing while $(s3 + s4)$ and $(s1 - s5)$ are geometric distances from point AB to B1, from AC to C1 and from Ao to B2 and C2, as illustrated in Fig. 1.

3. The torque due to the bending angles q_B and q_c, of the B and C respectively can be expressed as:

$$\boldsymbol{T}^{A/B} = K_{wb} q_B \boldsymbol{b}_1$$
$$\boldsymbol{T}^{A/C} = -K_w q_c \boldsymbol{c}_1 \quad (20)$$

where K_w is a spring constant which represents the bending elasticity of the wings.

4. The influence of a control force Fz, which is produced by the automatic pilot, is applied by a control surface deflection and acts at point A2 (Fig. 1). This force may be expressed as:

$$\mathbf{F}_c^{A2} = Q_d S_r C_{l\delta} \delta \mathbf{a}_2 \qquad (21)$$

where δ is a function of the pitch angle and pitch rate α and $\dot{\alpha}$:

$$\delta = \frac{1}{V^2}[C_{f1}\alpha + C_{f2}\dot{\alpha}] \qquad (22)$$

and $C_{l\delta}$, C_{f1} and C_{f2} are constants parameters of the auto-pilot.

When the velocity in N of A1, A2, B1,B2,C1, and C2 is derived, contribution of the active forces in Eqs. (14-23) to the generalized active forces can be obtained. Substitution of these generalized active forces and the generalized inertia forces in Kane's equations [3], leads to the equations of motion of the system. In the present work, these equations were derived and coded with the aid of *Autolev 3* software [4].

Analysis and Results

Simulation of the equations of motion was performed for an aircraft with the following parameters: Masses: m_A=50, m_B=m_C=1.5kg. Inertia: I_{A2}=10, I_{B1}=I_{B2}= 0.1, I_{C1}=I_{C2}=0.1kgm^2. Lengths: S1 = 0.14, S2=0.1, S3=0.6, S4=0.3, S5=0.05, S6=0.1 and S7=0.75 m. K_w = 2000N/rad

$Q_d / V^2 = 0.6\ kg/\mathrm{m}^3$, $S_r = 1\ m^2$, $C_r = 0.3\ m$

$C_{l\alpha}^{body} = 1$, $C_{l\alpha}^{wing} = 2.5$ and $C_{mq} = 5$.

In Fig 2, results are given for an initial pitch disturbance of 0.01 radian for a case where the auto-pilot control is not applied. Results are given for three velocities: 1. For V = Vf =96.3m/sec which is the critical flutter velocity for this set of parameters. 2. For V = 85 m/sec which is below the critical flutter velocity - thus the initial coupled vibrations decay. 3. For V= 105 m/sec which is above the critical speed - thus the coupled vibration amplitudes diverge. The increase of the frequency with the velocity can also be observed.

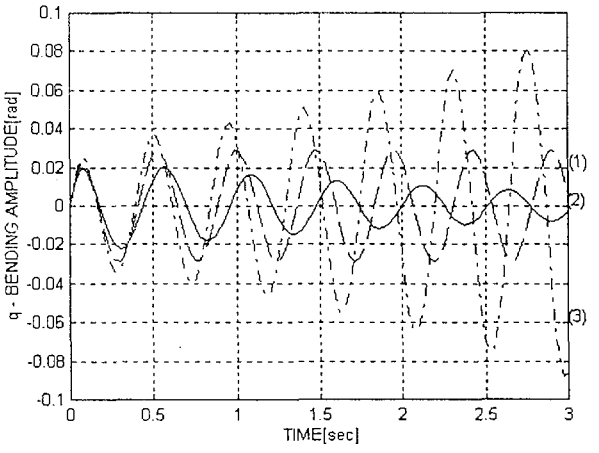

Fig. 2: Influence of velocity on the bending amplitude, for (1) - V=Vf=96.3, (2) - V=85 and (3) V= 105 m/sec

It can be clearly observed that the coupling between the pitch of the body and the bending of the wings depends directly on the distances S1 (see Fig. 1). As the distance S1 becomes larger, the coupling becomes stronger and thus Vf tends to become lower. On the other hand, when S1 is increased the pitch stability of the body (Fig. 1) is also increased and the damping on the wings (Eqs. 17) becomes larger. The total influence of S1 on the critical velocity Vf was found after linearization of the equations of motion was performed (also with the *Autolev 3* software). By examining the eigenvalues of the system, the critical flutter velocity can easily be determined. The results of this analysis are described in Fig 3 for the above mentioned set of parameters.

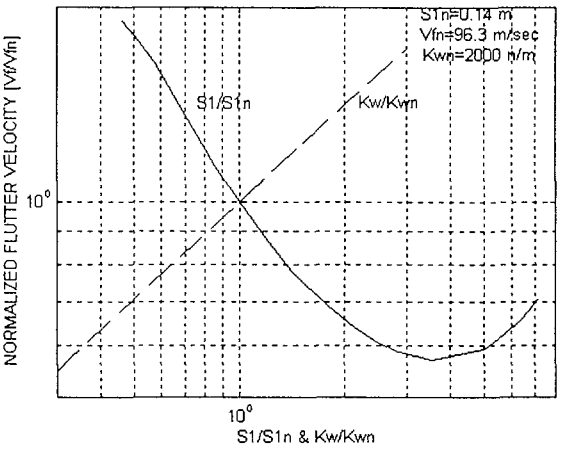

Fig 3: Influence of (1) S1 axial distance from body c.g. to wings c.g. (Fig. 1) and (2) K_w - wings bending constant on critical flutter speed Vf

The influence of the bending spring constant K_w on Vf is also represented in Fig. 3. In this case the increase of the critical flutter velocity is proportional to $\sqrt{K_w / K_{wn}}$ where K_{wn} is the nominal bending spring constant.

Fig. 4 shows the frequencies of the three modes as a function of the velocity V. At V equals zero (i.e. zero airspeed) the system oscillates in its two natural frequencies. One is the uncoupled bending mode of the wings of 9.1 Hz, while the second is the a body elevation mode coupled with wings flapping of 8.9 Hz. At V=0, the frequency of the coupled pitch/bending flutter mode is zero. It is seen that the frequencies of the first two modes decrease markedly with increase of V until they vanish at about V/Vf=0.6, while the flutter mode frequency increases with V.

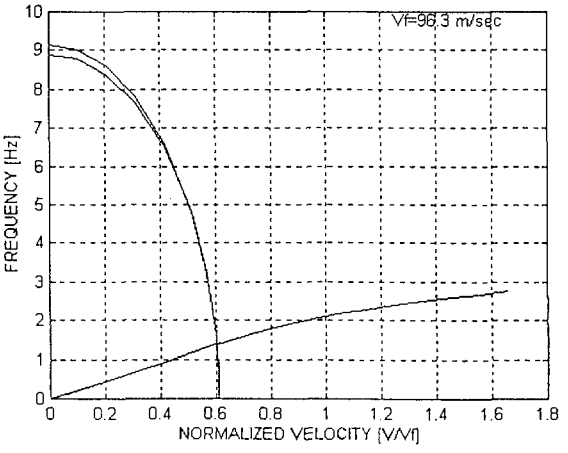

Fig 4 :Frequencies vs. velocity

The behavior of the system changes dramatically when the control force of the auto-pilot is added. The influence of the auto-pilot control force is to increase the rigidity of the body to pitch dynamics and to increase its damping. This influence is described in Fig. 5 for the following set of the auto-pilot parameters (Eqs. 21 and 22 and Fig 1): $S7$=0.75 m, V=105m/sec

$$C_{l\delta}^{body} = 0.5,\ C_{f1} = 2000\frac{\sec^2}{m^2} \text{ and } C_{f2} = 350\frac{\sec}{m^2}.$$

In this case without the auto-pilot the oscillation amplitudes diverge. Adding of the control force causes the amplitudes to decay.

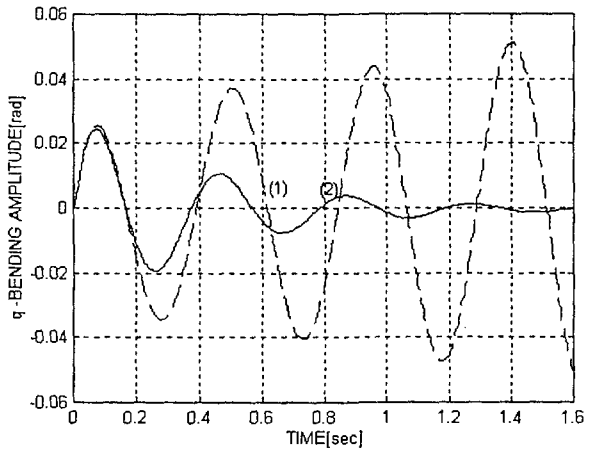

Fig. 5: Bending amplitudes (1) without control force and (2) with control force, at V=105m/sec

The resulting effect of the auto-pilot control force is to eliminate the unstable zone of the system. This phenomenon can be observed in Fig. 6 in which the real part of the flutter mode eigenvalue is described for the system with and without the control force (assuming that there is no change in the aerodynamic coefficients for the given velocity rang). It is clearly demonstrated that while for the uncontrolled conditions the system is unstable for V > 96.3 m/sec, (positive real part of the eigenvalue), the controlled system remains stable throughout the entire velocity range.

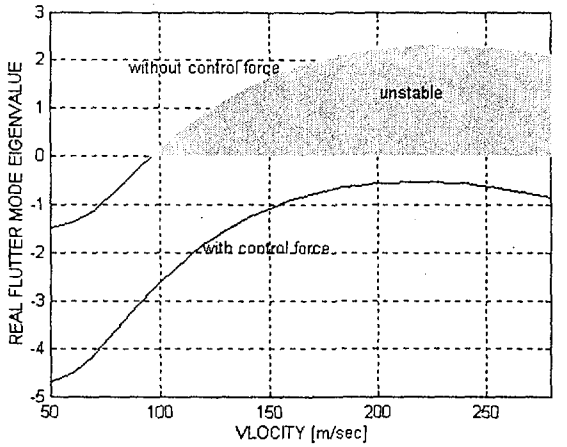

Fig. 6: Real part of flutter mode eigenvalue as a function of velocity, with and without the control force

Summary

A flutter phenomenon due to coupling between aircraft pitch and the bending of its wings was demonstrated. The influence of various parameters of the system on the critical flutter velocity was analyzed. It was shown that adding control forces of the auto-pilot might eliminate the instability zone of this flutter mode at the given set of the system parameters.

References

[1] Hancock G.J.,Wright J.R. and Simpson A., **On the Teaching of the Principle of Wing Flexure-Torsion Flutter,** Aeronautical Journal, October 1985, pp. 285-305.

[2] Yehezkely E. and Karpel M., **Nonlinear Flutter Analysis of Missile with Pneumatic Fin Actuator,** J. of Guidance, Control and Dynamics V. 19 No. 3 May/June 1966 pp. 664-670.

[3] Kane T.R. and Levison D. A., **Dynamics - Theory and Applications,** McGraw-Hill, 1985.

[4] Kane T.R. and Levinson A.L., **Dynamics Online - Theory and Implementation with AUTOLEV™.**, Online Dynamics Inc. Sunnyvale, CA 94087, 1995.